능동 전력 필터를 위한 새로운 디지탈 제어

○송 의호, 권 봉환
포항공대 전자전기 공학과

A Novel Digital Control for Active Power Filter

E.H. Song and B.H. Kwon
Dept. of Electronical and Electrical Eng., POSTECH

ABSTRACT

A novel digital control algorithms are developed for an active power filter (APF) using a pulse-width modulated (PWM) rectifier with current link. A main control algorithm compensating both the reactive power and harmonic currents with fast dynamic response is derived through a vector approach. A space vector modulation technique is developed for the PWM rectifier in order to generate the desired current vector of the APF. The system generates no acoustic noise and it is implemented with a minimal control hardware structure using the Intel 80196 single-chip microcomputer. Experimental results show that the proposed scheme gives good dynamic and static performance for the APF system.

I. INTRODUCTION

Nowadays, two problems are seriously considered in modern power electronic industry. One is a poor power factor due to the wide use of the inductive loads, *motors et al.* The other is polution of the utility grid due to the harmonic interference of the nonlinear loads (especially by power converters such as rectifiers, inverters and cycloconverters). This electro-magnetic interference (EMI), so called, has frequently been causing malfunctons of computer systems in the near of electrical equipments, and its restrictions are becomming more and more rigorous in the power electronic systems. Thyristor converters are widely used in industrial applications in these days and they can be considered as a typical example causing the afore-mentioned problems. Shunt passive filters have hitherto been used to solve the problems in power system. Active power filters have better harmonic compensation characteristics against both the impedance variation of ac power lines and the frequency variation of harmonic currents than conventional passive filters. So far, a voltage source PWM converter has usually used in the active power filters or in the VAR compensators [1] and [6]. A current source APF has an inductor with a constant dc current, whereas the voltage source APF has a capacitor on the dc side with a constant dc voltage. Although the voltage source type is better with regard to loss and the filter capacity to eliminate the PWM carrier harmonics, the current source type is better with regard to dynamics of the compensating current as well as reliability and protection [7].

Active power filters can be considered as rectifiers because its physical energy resource results from not dc side but ac side. In general, three techniques are available to control the current waveform of PWM rectifiers; there are hysteresis, sinusoidal, and space vector PWM control. The hysteresis PWM control is simple, but its average switching frequency varies with the load condition so that the switching pattern is uneven and random. The sum of the three-phase current must be zero when neutral is not connected. This means that the current flowing in any phase depends on the state of the other two phases. Since the hysteresis and sinusoidal PWM control are three phase independent control, no account is taken of this relation of phases in the current control algorithm. On the other hand, in the space vector modulation technique, this relation of phases is taken of account introducing the state space vector concept [8] and [9]. The major characteristics of the space vector modulation technique are that the maximum modulation index and the number of switching are 15 percent larger and 30 percent less than the one obtained by sinusoidal PWM, respectively, the synchronization of carrier to signal wave is not needed, and on-line PWM control

using a single-chip microcomputer is possible.

In this paper, a new approach to solve the afore-mentioned two problems is presented as a control scheme for the APF system. The control block of the APF consists of four parts, namely, the sensing block, the main compensation block, the control block for the dc link current, and PWM pulse generation block. The system generates no acoustic noise and it is implemented with a minimal control hardware structure using the Intel 80196 single-chip microcomputer. Experimental results show that the proposed scheme compensates both the reactive power and harmonic currents with extremely fast dynamic response.

II. System Configuration and Compensation Principle

Fig. 1 shows a system configuration of the active power filter which was installed for compensating both the reactive power and harmonic currents generated by the 6-pulse phase-controlled rectifier (PCR). The active power filter system consists of a PWM rectifier with current link and a single-chip microcomputer as its controller. The filter capacitance C are used to suppress switching ripples generated by the APF. The compensating current i_r of the APF with current link has more fast dynamics than that of the APF with voltage link.

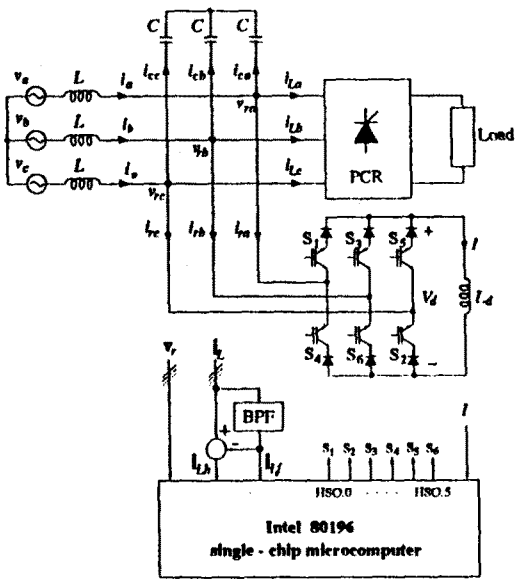

Fig. 1. Fully software-controlled active power filter using one single-chip microcomputer.

The control block in the sigle-chip microcomputer consists of four parts, namely, the sensing block, the main compensator block, the dc link current control block, and PWM pulse generation block. The load current is decomposed to fundamental component and harmonic component by the band-pass filter (BPF). In the sensing block, the feedback data such as source voltage, fundamental load current, harmonic load current and dc link current I are read into the microcomputer through an 8-channel A/D converter. Using the well-known power invariant transform, instantaneous three phase quantities can uniquely be represented by components of real and imaginary axes in the fixed frame. The represented vectors rotates with angular velocity ωt in this frame. The main compensator block produces signals for the PWM pulse generation block and dominates directly the compensation characteristics of the active power filter. The direction of source voltage is defined as an active axis and its orthogonal direction is a reactive axis. Then, the poor power factor of the PCR can be improved by canceling the reactive component of the fundamental load current. The harmonic interference can be removed by canceling harmonic components of load current. Thus the main control algorithm of the active power filter is derived. The control algorithm of the dc current is derived from an active power flow in the energy storage element L_d. The command of the dc current is only reconstructed from feedback signals to close of the loop around the active power filter system. Since the compensationg current of the APF is also obtained as a vector form, it is desirable to implement this without transforming two axis quantities to three phase quantities. In the PWM pulse generation block, a space vector modulation technique is developed to generate PWM signal.

III. Controller Design

The APF is to compensate the reactive and harmonic components of the load current so that the source current i may only consist of an active component, that is, in-phase current with the source voltage. A schematic diagram of the APF system is shown in Fig. 2 with functional descriptions.

A. Main Compensator

Tne main compensator is designed using the developed concepts in the Section II. To compensate the harmonic component of the load current, choose that

$$i_{rh} = -i_{Lh}. \tag{1}$$

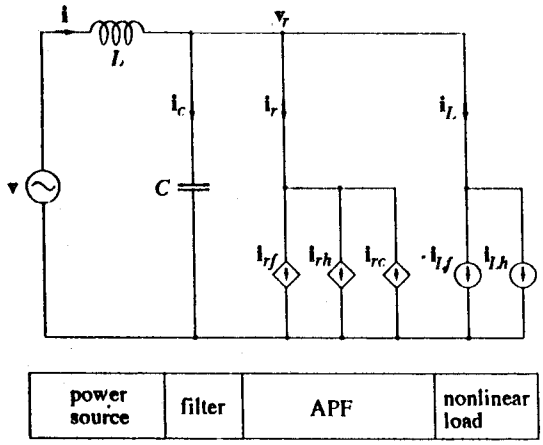

Fig. 2. Schematic diagram of APF system.

To compensate the reactive component of the fundamental load current, choose that

$$I_{rfm} = I_{Lfm} \sin \phi_{iLf} - I_{cm} \cos \phi_{vr}. \quad (2)$$

This result is induced from the vector diagram in Fig. 3. Then

$$\begin{aligned} \mathrm{i}_{rf} &= I_{rfm} \exp j(\omega t + \pi/2) \\ &= j \sin \phi_{iLf} I_{Lfm} \exp j\omega t - j \cos \phi_{vr} I_{cm} \exp j\omega t. \end{aligned} \quad (3)$$

Using identities that

$$I_{Lfm} \exp j\omega t = \mathrm{i}_{Lf} \exp j\phi_{iLf} \quad (4)$$

$$I_{cm} \exp j\omega t = \omega C \mathrm{v}_r \exp j\phi_{vr}, \quad (5)$$

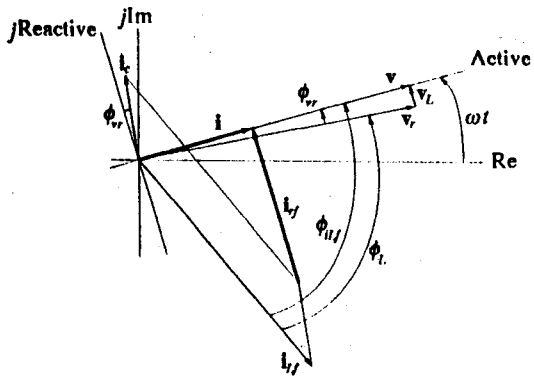

Fig. 3. Compensation principle of the fundamental load current by APF.

fundamental phase current of the APF is obtained as

$$\mathrm{i}_{rf} = j \sin \phi_{iLf} \mathrm{i}_{Lf} \exp j\phi_{iLf} - j \cos \phi_{vr} \omega C \mathrm{v}_r \exp j\phi_{vr}. \quad (6)$$

If the source inductanc L is neglizable, we can assume that

$$\phi_{vr} = 0 \quad (7)$$

$$\phi_{iLf} = \phi_L. \quad (8)$$

Substituting (7) and (8) into (6), the phase current of APF is obtained as follows:

$$\begin{aligned} \mathrm{i}_{rf} + \mathrm{i}_{rh} &= j \sin \phi_{iLf} \mathrm{i}_{Lf} \exp j\phi_{iLf} \\ &\quad - j \cos \phi_{vr} \omega C \mathrm{v}_r \exp j\phi_{vr} - \mathrm{i}_{Lh}. \end{aligned} \quad (9)$$

By the reference frame theory, balanced three phase data can be converted to two orthogonal components as

$$\mathrm{v} = v_x + j v_y. \quad (10)$$

Applying similar relations to (9), the following equation is derived

$$\begin{bmatrix} i_{rfx} + i_{rhx} \\ i_{rfy} + i_{rhy} \end{bmatrix} = \begin{bmatrix} -\sin^2 \phi_L & -\frac{1}{2} \sin 2\phi_L \\ \frac{1}{2} \sin 2\phi_L & -\sin^2 \phi_L \end{bmatrix} \begin{bmatrix} i_{Lfx} \\ i_{Lfy} \end{bmatrix} + \begin{bmatrix} 0 & \omega C \\ \omega C & 0 \end{bmatrix} \begin{bmatrix} v_{rx} \\ v_{ry} \end{bmatrix} - \begin{bmatrix} i_{Lhx} \\ i_{Lhy} \end{bmatrix} \quad (11)$$

From this, the compensator of the load current, heart of the APF, is built up in Fig. 4. The functions in this figure can be fully implemented by the sigle-chip microcomputer, the Intel 80196.

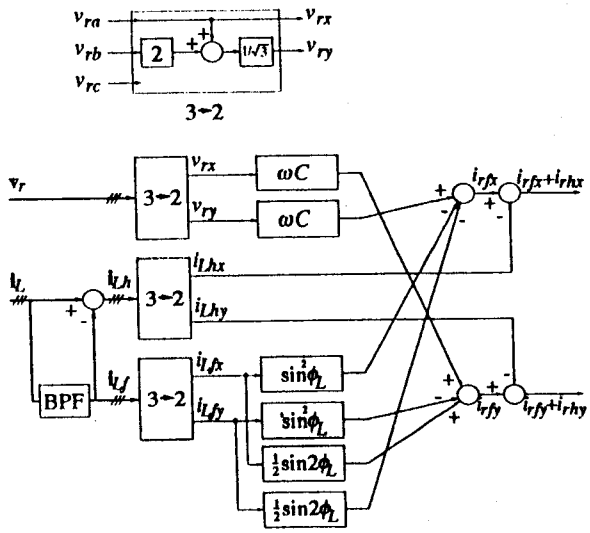

Fig. 4. Compensation of the reactive and the harmonic current by APF.

B. Dc Link Current Controller

The dc link current I of APF is to supply two power components. One is lossless power that is charged in the inductance L_d to generate desired phase current of the APF.

The other is lossy power due to the switching loss and the resistive. Its phase current i_{rc} must be in-phase with the source voltage in order to be active power. With this idea, an inner dc link current control loop is presented in Fig. 5.

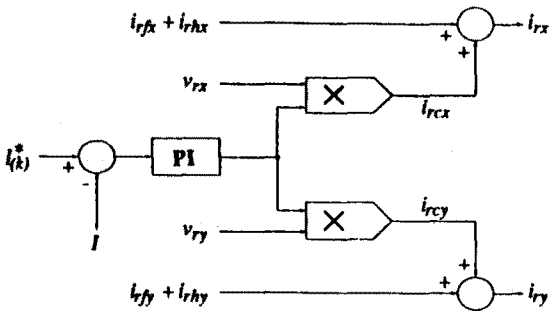

Fig. 5. Dc current controller of the APF.

C. Dc Current Reference Generation

The dc current reference of the inner loop, $I_{(k)}^*$, can be contained in the total system loop. The desired phase current of the APF, i_r, depends on the load and is given by (9). The dc current of the APF, I, should be adjusted so as to supply the phase current. Moreover, it should keep up more than the maximum value of the desired phase current to guarantee stable operation of the APF system. Thus, an absolute value of the desired phase current is considered as follows:

$$\begin{aligned} |i_r| &= |j \sin\phi_{iLf} i_{Lf} \exp j\phi_{iLf} - j \cos\phi_{vr} \omega C v_r \exp j\phi_{vr} - i_{Lh}| \\ &\le |j \sin\phi_{iLf} i_{Lf} \exp j\phi_{iLf}| + |j \cos\phi_{vr} \omega C v_r \exp j\phi_{vr}| + |i_{Lh}| \\ &\le |\sin\phi_{iLf}||i_{Lf}| + \omega C |\cos\phi_{vr}||v_r| + |i_{Lh}|. \end{aligned} \quad (12)$$

From this inequalities and the approximations (7) and (8), the dc current reference of the outer loop, I^*, is given by

$$I^* = |\sin\phi_L||i_{Lf}| + \omega C|v_r| + |i_{Lh}|. \quad (13)$$

The marginal I^* is added to fill up the switching and the resistive losses, but the heavier margin brings about the more swiching loss. With these discussions, the dc current reference is generated in Fig. 6. In this figure, the (max. det.) detects maximal absolute values by checking when the y component is approximately zero. A PI controller with slower dynamics than inner loop is included to form an outer regulation loop.

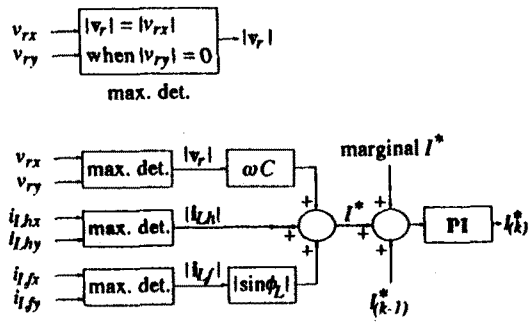

Fig. 6. Dc current reference generation of the APF.

IV. PWM Scheme of the Active Power Filter

The desired ac current of the APF, i_r, has been obtained in Section III and it can be implemented through various PWM techniques. Aactive power filters be considered rectifier systems because its physical energy resource results from not dc side but ac source side. The main circuit of the PWM rectifier with current link is shown in Fig. 1.

A. State Space Vectors

A dc current link rectifier/inverter system has an inductor on the dc side and capacitors on the phase side of the bridge. Its two constraints are as follows:

- There must always exist a current path for the dc current.
- There must be no short circuit between ac phase.

These constraints can be mathematically represented by

$$d_1^* + d_3^* + d_5^* = 1 \quad (14)$$

$$d_4^* + d_6^* + d_2^* = 1 \quad (15)$$

where the switching function d_k^* is

$d_n^* = 1$ when switch n is on

$d_n^* = 0$ when switch n is off.

The rectifier with dc current link can produce only six current space vectors $\mathbf{I}_{1-6}$ in the range space and three zero current vectors $\mathbf{I}_{7-9}$ in the null space. The quantized current space vectors are given as follows:

$$\mathbf{I}_n = \frac{2}{\sqrt{3}} I \exp\{j(2n-1)\frac{\pi}{6}\},$$

$$\text{for } n = 1, 2, \cdots, 6 \qquad (16)$$

$$\mathbf{I}_n = 0, \quad \text{for } n = 7, 8, 9. \qquad (17)$$

These space vectors are called as state space vectors of the current which are shown in Table I and in Fig. 7. The desired current space vector $\mathbf{i}_r$ can be expressed by combining the state space vectors in (16) and (17) with appropriate weighting functions.

Table I: Switch combinations of the PWM rectifier with current link

	Range space						Null space		
	$\mathbf{I}_1$	$\mathbf{I}_2$	$\mathbf{I}_3$	$\mathbf{I}_4$	$\mathbf{I}_5$	$\mathbf{I}_6$	$\mathbf{I}_7$	$\mathbf{I}_8$	$\mathbf{I}_9$
S_1	1	0	0	0	0	1	1	0	0
S_2	1	1	0	0	0	0	0	0	1
S_3	0	1	1	0	0	0	0	1	0
S_4	0	0	1	1	0	0	1	0	0
S_5	0	0	0	1	1	0	0	0	1
S_6	0	0	0	0	1	1	0	1	0
i_a	I	0	-I	-I	0	I	0	0	0
i_b	0	I	I	0	-I	-I	0	0	0
i_c	-I	-I	0	I	I	0	0	0	0

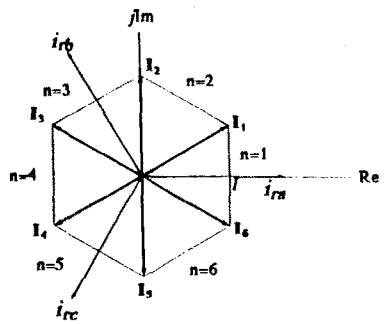

Fig. 7. State space vectors.

B. Waiting Functions and Switching Function

The desired space vector $\mathbf{i}_r$ is weighted in the sector n=1 as follows:

$$\mathbf{i}_r = w_6\mathbf{I}_6 + w_1\mathbf{I}_1 + w_7\mathbf{I}_7 \qquad (18)$$

where w_6 and w_1 denote the weigting functions of the two adjacent state space vectors $\mathbf{I}_6$ and $\mathbf{I}_1$, respectively. The zero state space vector $\mathbf{I}_7$ has been selected in sector n=1 because S_1 is the common factor of state space vectors $\mathbf{I}_6$ and $\mathbf{I}_1$. This weghting of the state space vectors is also called as a space vector modulation and it is shown in Fig. 8. The state space vectors $\mathbf{I}_6$, $\mathbf{I}_1$ and $\mathbf{I}_7$ can be represented with respect to the fixed real and imaginary coordinates in the sector n=1 as

$$\mathbf{I}_6 = \frac{2}{\sqrt{3}} I(\cos\frac{\pi}{6} - j\sin\frac{\pi}{6}) \qquad (19)$$

$$\mathbf{I}_1 = \frac{2}{\sqrt{3}} I(\cos\frac{\pi}{6} + j\sin\frac{\pi}{6}) \qquad (20)$$

$$\mathbf{I}_7 = 0 \qquad (21)$$

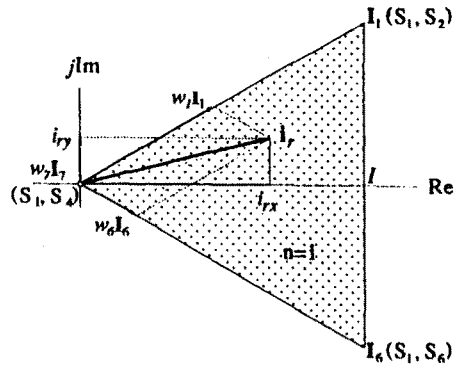

Fig. 8. Space vector modulation (sector n=1).

Substituting (19) and (21) to (18), the weighting functions w_6 and w_1 are derived as follows:

$$w_6 = \frac{1}{2I}(i_{rx} - \sqrt{3}i_{ry}) \qquad (22)$$

$$w_1 = \frac{1}{2I}(i_{rx} + \sqrt{3}i_{ry}). \qquad (23)$$

Then, the weighting function of the zero state space vector is

$$w_7 = 1 - w_6 - w_1. \qquad (24)$$

C. Switching Function

In the frequency range much lower than the switching frequency, the switching functions can be represented as

$$d_n = \frac{T_n}{T_s} \quad \text{for } n = 1, 2, \cdots, 6 \qquad (25)$$

where T_s is the switching period and T_n is on time of the indexed switch. The weighting functions are transformed to switching functions using two constraints of the dc current link rectifier and (22) - (24). An illustrative time chart is shown in Fig. 9, considering the example in Fig. 8. In the sector n=1, it should be noted that the S_1 remains on state for all time. Thus, the S_1 is selected as one of the upper leg switches. The constraints make the others to be selected in

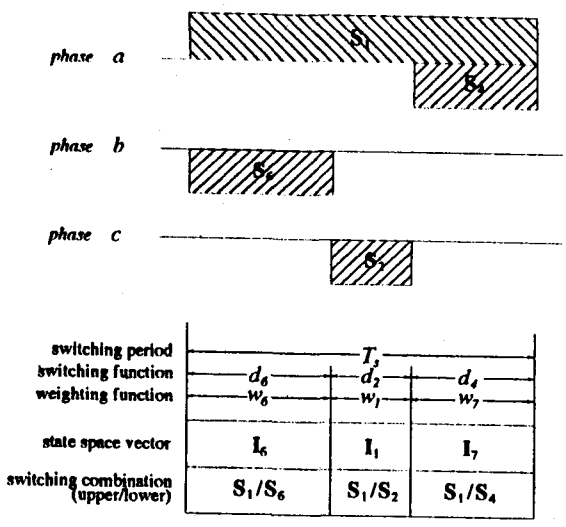

Fig. 9. Time chart of the switching functions (sector n=1).

the lower leg. In the border of the sector n=1, the switches S_6 and S_2 of the lower leg are seclected for the weighting functions w_6 and w_1, respectively. The conducting time of these switches should be distributed in the switching period with no intersection because of the constraints. The remaining switch of the lower leg should be the complement of S_1. Thus, S_4 is selected for the weighting functions w_7 related with the zero state space vector. From the selected switches, the transformations to switching functions are completed in the sector n=1 as follows:

$$d_1 = 1, \quad d_3 = 0, \quad d_5 = 0$$
$$d_6 = w_6 = \frac{1}{2I}(i_{rx} - \sqrt{3}i_{ry}) \qquad (26)$$
$$d_2 = w_1 = \frac{1}{2I}(i_{rx} + \sqrt{3}i_{ry})$$
$$d_4 = w_7 = 1 - d_6 - d_2.$$

This concept can be directly applied for all sectors. Table II shows switching functions of the six switches in all sectors. It is very complex to implement these switching functions using the conventional sinusoidal PWM control technique. However, it will be an useful tool when the desired phase current of the rectifier, i_r, is given by two orthogonal components.

C. Sector Finder

Considering implementation problem, the switching functions of the Table II should be positive. This requires an algorithm, sector finder, in which the line current of the PWM rectifier uniquely fall down to one sector except on boundaries of the sectors. It is shown in Fig. 10 that the algorithm is developed by considering the sign and the magnitude of the desired phase current i_r.

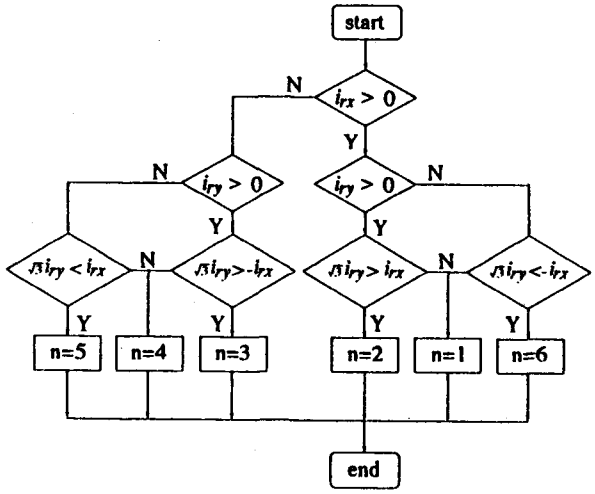

Fig. 10. Sector finding algorithm.

Table II: Switching functions of the six switches

	n=1	n=2	n=3	n=4	n=5	n=6
d_1	1	$\frac{i_{rx}}{I}$	0	$1-d_3-d_5$	0	$\frac{i_{rx}}{I}$
d_2	$\frac{i_{rx}+\sqrt{3}i_{ry}}{2I}$	1	$\frac{i_{rx}+\sqrt{3}i_{ry}}{2I}$	0	$1-d_4-d_6$	0
d_3	0	$\frac{-i_{rx}+\sqrt{3}i_{ry}}{2I}$	1	$\frac{-i_{rx}+\sqrt{3}i_{ry}}{2I}$	0	$1-d_5-d_1$
d_4	$1-d_6-d_2$	0	$-\frac{i_{rx}}{I}$	1	$-\frac{i_{rx}}{I}$	0
d_5	0	$1-d_1-d_3$	0	$\frac{-i_{rx}-\sqrt{3}i_{ry}}{2I}$	1	$\frac{-i_{rx}-\sqrt{3}i_{ry}}{2I}$
d_6	$\frac{i_{rx}-\sqrt{3}i_{ry}}{2I}$	0	$1-d_2-d_4$	0	$\frac{i_{rx}-\sqrt{3}i_{ry}}{2I}$	1

IV. Conclusions

In this paper, an active power filter with a minimal control hardware structure is presented. A main algorithm is derived through a vector approach compensating both the reactive power and the harmonic currents effectively. When the desired phase current is given by a vector form, a space vector modulation technique is developed for a PWM rectifier with current link . The control algorithm of the dc current is derived from the flow of real power in the energy storage element. The command of the dc link current is only generated from feedback signals to close of the loop around the active power filter system. All of the control functions can be implemented with a single-chip microcomputer, the Intel 80196.

References

[1] F.Z. Peng, H. Akagi and A. Nabae, "A New approach to harmonic compensation in power systems - A combined system of shunt passive and series active filters,"*IEEE Trans. Ind. Appl.*, vol. IA-26, no. 6, pp. 983-990, Nov./Dec. 1990.

[2] H. Akagi, Y. Kanazawa and A. Nabae, "Instantaneous reactive power compensators comprising switching devies without energy storage components,"*IEEE Trans. Ind. Appl.*, vol. IA-20, no. 3, pp. 625-630, May./June 1984.

[3] T. Furuhashi, S. Okuma and Y. Uchikawa, "A study on the theory of instantaneous reactive power," *IEEE Trans. Ind. Electron.*, vol. IE-37, no. 1, pp. 86-90, Feb. 1990.

[4] H. Akagi, Y. Kanazawa and A. Nabae, "Analysis and design of an active power filter using quad-series voltage source PWM converters,"*IEEE Trans. Ind. Appl.*, vol. IA-26, no. 1, pp. 93-98, Jan./Feb. 1990.

[5] M. Matsui and T. Fukao, "A detecting method for active-reactive-negative-sequence powers and its application,"*IEEE Trans. Ind. Appl.*, vol. IA-26, no. 1, pp. 99-106, Jan./Feb. 1990.

[6] G. Joos, L. Moran and P. Ziogas, "Performance analysis of a PWM inverter Var compensator," *IEEE Trans. Power Electron.*, vol. PE-6, no. 3, pp. 380-391, July 1991.

[7] Y. Hayashi, N. Sato and K. Takahashi, " A novel control of a current-source active filter for ac power system harmonic compensation,"*IEEE Trans. Ind. Appl.*, vol. IA-27, no. 2, pp. 380-385, Mar./Apr. 1991.

[8] S. Fukuda, Y. Iwaji and H. Hasegawa, "PWM technique for inverter with sinusoidal output current," *IEEE Trans. Power Electron.*, vol. PE-5, no. 1, pp. 54-61, Jan. 1990.

[9] G. Ledwich, "Current source inverter modulation," *IEEE Trans. Power Electron.*, vol. PE-6, no. 4, pp. 618-623, Oct. 1991.

[10] J.W. Dixon and B.T. Ooi, "Indirect current control of a unity power sinusoidal current boost type three-phase rectifier," *IEEE Trans. Ind. Electron.*, vol. IE-35, no. 4, pp. 508-515, Nov. 1988.

[11] G.H. Choe and M.H. Park, "Analysis and control of active power filter with optimized injection," *IEEE Trans. Power Electron.*, vol. PE-4, no. 4, pp. 427-433, Oct. 1989.

[12] Intel Embedded Controller Handbook, Intel Corp., 1987.